Published in final edited form as:
Cell. 2014 March 13; 156(6): 1223–1234. doi:10.1016/j.cell.2014.01.069.

Heme-mediated SPI-C induction promotes monocyte differentiation into iron-recycling macrophages

Malay Haldar[1], **Masako Kohyama**[2], **Alex Yick-Lun So**[3], **KC Wumesh**[1], **Xiaodi Wu**[1], **Carlos G. Briseno**[1], **Ansuman T. Satpathy**[1], **Nicole M. Kretzer**[1], **Namakkal Soorappan Rajasekaran**[4], **Li Wang**[5], **Takeshi Egawa**[1], **Kazuhiko Igarashi**[6], **David Baltimore**[3], **Theresa L. Murphy**[1], and **Kenneth M. Murphy**[1,7,*]

[1]Department of Pathology and Immunology, Washington University in St. Louis, School of Medicine, St. Louis, Missouri 63110, USA

[2]Laboratory of Immunochemistry, WPI Immunology Frontier Research Center, Osaka University, Suita, Osaka 565–0871, Japan

[3]Department of Biology, California Institute of Technology, Pasadena, California 91125, USA

[4]Division of Cardiology & Pulmonary, Department of Internal Medicine, University of Utah Health Sciences Center, Salt Lake City, Utah 84132, USA

[5]Division of Gastroenterology, Department of Internal Medicine, University of Utah Health Sciences Center, Salt Lake City, Utah 84132, USA

[6]Department of Biochemistry, Tohoku University Graduate School of Medicine, Sendai 980-8575, Japan

[7]Howard Hughes Medical Institute, Washington University in St. Louis, School of Medicine, St. Louis, Missouri 63110, USA

Abstract

Splenic red pulp macrophages (RPM) degrade senescent erythrocytes and recycle heme-associated iron. The transcription factor *Spic* is selectively expressed by RPM and is required for their development, but the physiologic stimulus inducing *Spic* is unknown. Here, we report that *Spic* also regulated the development of F4/80^{+}VCAM1^{+} bone marrow macrophages (BMM) and that *Spic* expression in BMM and RPM development was induced by heme, a metabolite of erythrocyte degradation. Pathologic hemolysis induced loss of RPM and BMM due to excess heme but induced *Spic* in monocytes to generate new RPM and BMM. *Spic* expression in monocytes was constitutively inhibited by the transcriptional repressor *Bach1*. Heme induced proteasome-dependent BACH1 degradation and rapid *Spic* derepression. Furthermore, cysteine-proline dipeptide motifs in BACH1 that mediate heme-dependent degradation were necessary for

*To whom correspondence should be addressed. Phone 314-362-2009, Fax 314-747-4888, kmurphy@wustl.edu.

Spic induction by heme. These findings are the first example of metabolite-driven differentiation of a tissue-resident macrophage subset and provide new insights into iron homeostasis.

Introduction

Macrophage function extends beyond immunity to include roles in embryonic development, wound repair, and local tissue homeostasis (Pollard, 2009; Murray and Wynn, 2011). Macrophages in various tissues have distinct tissue-specific homeostatic roles such as osteoclasts that regulate bone morphogenesis, alveolar macrophages that regulate pulmonary surfactant turnover, and splenic red pulp macrophages (RPM) that regulate erythrocyte degradation and iron recycling (Pollard, 2009; Gordon and Taylor, 2005; Taylor et al., 2005; Murray and Wynn, 2011; Marks, Jr. and Lane, 1976; Cecchini et al., 1994; Shibata et al., 2001; Dranoff et al., 1994; Kohyama et al., 2009). These tissue-resident macrophages are thought to be maintained by the differentiation of circulating monocytes and local proliferation (Landsman and Jung, 2007; Jenkins et al., 2011; Hume, 2008). Recently, a subset of tissue-resident macrophages have been shown to arise from cells in the primitive ectoderm of the yolk sac without a monocytic intermediate (Schulz et al., 2012a). However, factors controlling the relative contribution of yolk sac-derived and monocyte-derived macrophages are unknown.

RPM, and to some extent bone marrow macrophages (BMM) and liver macrophages, phagocytose senescent or damaged erythrocytes to degrade heme and release the heme-associated iron (Ganz, 2012; Beaumont and Delaby, 2009). Iron is an essential element required for many critical biological processes (Pantopoulos et al., 2012). The majority of iron in the body is contained within the heme moiety of hemoglobin inside erythrocytes, and each day about 3.6×10^{11} erythrocytes are recycled by the aforementioned macrophage-dependent pathway, supplying the vast majority of the daily iron requirement (Andrews and Schmidt, 2007; Ganz, 2012; Pantopoulos et al., 2012; Bratosin et al., 1998). Given the proficiency of RPM and BMM in erythrophagocytosis, these cells experience significant increases in heme following erythrocyte damage in pathological conditions such as autoimmune hemolytic anemia, drug or toxin induced hemolysis, and sickle cell disease (Guillaud et al., 2012). However, very high levels of intracellular heme is toxic to these cells as demonstrated by the elimination of RPM and BMM upon inactivation of the heme-degrading enzyme heme oxygenase 1 (*Ho1*) (Kovtunovych et al., 2010). Indeed, excess intracellular heme is toxic to macrophages even with intact *Ho1* (Cambos and Scorza, 2011). Therefore, conditions leading to increased heme levels may require ‘replenishment’ of the RPM and BMM population to maintain iron homeostasis.

We have previously reported the requirement of the transcription factor *Spic* for the development of RPM (Kohyama et al., 2009). To examine the signals controlling *Spic* induction and RPM development *in vivo*, we targeted enhanced green fluorescent protein (EGFP) for expression under the control of the native *Spic* locus. Our analysis demonstrated that it is the heme moiety derived from senescent or damaged erythrocytes that is the physiologic trigger for inducing *Spic*. This induction appeared to take place in a subset of monocytes and proceeds by the heme-mediated degradation of BACH1 protein, a

transcriptional repressor that inhibited *Spic* under normal conditions. We found that *Spic* also regulated BMM that phenotypically resembled RPM, and that the heme-*Bach1-Spic* circuit induced compensatory development of RPM and BMM during pathological hemolysis. These findings uncover a novel metabolite-driven pathway regulating tissue-specific macrophage development and provide new insights into iron homeostasis.

Results

Spic is required for the development of F4/80^{hi} macrophages in the spleen and bone marrow

Spic is a member of the Spi subfamily of ETS transcription factors and is required for the development of RPM (Bemark et al., 1999; Carlsson et al., 2002; Kohyama et al., 2009). To examine *Spic* regulation, we generated a *Spic*^{igfp} allele by inserting an internal ribosomal entry site (IRES) and EGFP expression cassette immediately downstream of the *Spic* gene stop codon (Figures S1A and S1B). This strategy does not disrupt the endogenous *Spic* coding sequence and allows tracking of SPIC protein expression in the context of normal RPM development. *Spic*$^{igfp/+}$ and *Spic*$^{igfp/igfp}$ mice were born at Mendelian frequency and developed normally, and had normal development of RPM (Figure S1C). SPIC-EGFP^{+} splenocytes expressed significantly more *Spic* transcripts compared to SPIC-EGFP^{-} splenocytes in *Spic*$^{igfp/+}$ mice, indicating that the EGFP levels reflects endogenous *Spic* transcription (Figure S1D).

As expected, EGFP levels were high in RPM (Figures 1A and 1B). We also observed high levels of EGFP in F4/80^{hi} cells in the bone marrow (BM) (Figures 1A and 1B) and in a small fraction of F4/80^{hi} cells in the liver, but not at other locations (Figure S2A). SPIC-EGFP^{hi} cells in the BM expressed low levels of the myeloid marker CD11b but were neither neutrophils (Ly6G^{hi}) nor monocytes (Ly6C^{hi}) (Figure 1C). However, these SPIC-EGFP^{hi} BM cells expressed high levels of macrophage-associated markers including F4/80, VCAM1, CD68, and CD169, supporting their identity as BM-macrophages (BMM) (Figure 1C). Furthermore, SPIC-EGFP ^{hi} BMM displayed a striking similarity to RPM (Kohyama et al., 2009; Hemmi et al., 2009), with both cells being CD11b^{lo} MHCII^{int} VCAM1^{hi} TREML4^{hi} (Figures S2B–S2E). BMM and RPM were negative for the dendritic cell-specific marker *Zbtb46* (Satpathy et al., 2012) and dendritic cells did not express SPIC-EGFP (Figure S2F). These results demonstrated that *Spic* is expressed at high levels in both BMM and RPM suggesting a common developmental origin for these macrophage subsets. Indeed, *Spic*$^{-/-}$ mice were found to be deficient in F4/80^{hi} VCAM1^{hi} BMM in addition to the previously reported loss of RPM (Figure 1D). Macrophages in other locations surveyed were present in normal numbers (Figure S2G).

SPIC-EGFP ^{hi} BMM were F4/80^{hi}VCAM1^{hi}CD11b^{lo}CD169^{+}CD68^{+} (Figures 1C), which is similar to the reported surface marker profile of the previously described CD169 $^{+}$ BMM (Chow et al., 2011; Chow et al., 2013). CD169 expression was significantly decreased in *Spic*$^{-/-}$ BM indicating loss of these macrophages (Figure 1E). CD169^{+} BMM have been suggested to support normal erythropoesis in the BM (Chow et al., 2013). Proerythroblast frequencies were reduced in the BM of *Spic*$^{-/-}$ mice that is consistent with the reported phenotype (Chow et al., 2013) upon ablating CD169^{+} BMM (Figure 1F). Furthermore,

hemoglobin recovery from hemolytic anemia appeared impaired, albeit not statistically significantly, in *Spic*$^{-/-}$ mice (Figure S2H). Taken together, these results demonstrated the role of *Spic* in regulating the development of F4/80^{hi}VCAM1^{hi}CD169^{+} BMM.

Heme induces Spic expression in macrophages generated in vitro

We next considered factors that may induce *Spic* expression to promote RPM and BMM development. Several potential RPM-specific transcription factors failed to induce SPIC-EGFP in macrophages generated *in vitro* by culturing *Spic*$^{igfp/igfp}$ bone marrow cells in the presence of GM-CSF (BM-derived macrophages, BMDM). Retroviral expression of *Spic* in BMDM did not induce SPIC-EGFP, arguing against auto-activation, and neither did *Tcfec*, which encodes another RPM-associated transcription factor (Figure S3A). Agonist-mediated activation of the nuclear receptors NR1D1, PPARγ, LXRα, and RXRα (Heng and Painter, 2008), which are each highly expressed in RPM, also failed to induce SPIC-EGFP (Figure S3B–S3D).

Since RPM and BMM have characteristically high levels of intracellular heme, we next asked whether heme itself might induce *Spic*. Indeed, heme (Hemin, Sigma-Aldrich) selectively induced SPIC-EGFP in F4/80^{+} macrophages and Ly6C^{+} monocytes, but not in Ly6G^{+} neutrophils, in BM cultures (Figures 2A, 2B, and S4A). Heme-induced *Spic* expression was confirmed by reverse transcription PCR and was dose-dependent (Figure 2C).

The enzyme HO1 converts heme to biliverdin releasing the heme-associated iron while the enzyme biliverdin reductase (BLVR) converts biliverdin to bilirubin (Beaumont and Delaby, 2009). Thus, heme-induced *Spic* expression could be mediated by heme itself or one of these heme metabolites. Bilirubin and biliverdin failed to induce SPIC-EGFP in *Spic*$^{igfp/igfp}$ BMDM (Figure 2D). Furthermore, iron chelation by deferoxamine or HO1 inhibition by chromium mesoporphyrin (Crmp) (Schulz et al., 2012b) failed to inhibit heme-mediated SPIC-EGFP induction (Figures S4B and S4C). These results argue against a role of heme metabolites in *Spic* induction. We further confirmed this interpretation by genetic analysis. *Ho1*$^{-/-}$ mice were obtained (Poss and Tonegawa, 1997a) to generate *Ho1*$^{-/-}$ *Spic*$^{igfp/igfp}$ mice. Heme induced SPIC-EGFP expression in *Ho1*$^{-/-}$ *Spic*$^{igfp/igfp}$ BMDM (Figure 2E). Notably, BMDM were increasingly sensitive to heme-mediated *Spic* induction with loss of each allele of *Ho1* (Figure 2E). These results further demonstrate a direct role of heme in *Spic* induction.

Heme induces Spic expression in a subset of myeloid cells in vivo

Ho$^{-/-}$ mice have been previously reported to lack RPM and BMM (Kovtunovych et al., 2010). We noticed that lack of RPM and BMM in *Ho1*$^{-/-}$*Spic*$^{igfp/igfp}$ was associated with a significant increase in cells expressing low levels of SPIC-EGFP and the myeloid lineage marker CD11b (CD11b^{hi} SPIC-EGFP ^{lo} cells) in the spleen and BM, but not in other locations (Figures 3A and S5A). HO1 inhibition by Crmp also increased the number of CD11b^{hi} SPIC-EGFP $_{lo}$ cells while reducing RPM numbers *in vivo* (Figure 3B). Additionally, induction of intravascular hemolysis by phenylhydrazine (PDZ) (Itano et al., 1975; Chow et al., 2013) recapitulated this phenomenon (Figures 3C and S5B). Notably,

within the spleen these CD11b^{hi} SPIC-C-EGFP ^{lo} cells were located in the red pulp area similar to RPM (Figure 3D). These findings suggest a role of heme in the generation of CD11b^{hi} SPIC-EGFP ^{lo} cells *in vivo*.

Loss of RPM in *Ho1*$^{-/-}$ mice is thought to be due to heme-induced toxicity (Kovtunovych et al., 2010; Poss and Tonegawa, 1997b). Consistent with this, higher levels of heme induced the loss of *Ho1*$^{-/-}$*Spic*$^{igfp/igfp}$ BMDM (Figure 3E). Cell death was induced within 24 hours of exposure to high levels of heme in *Ho1*$^{-/-}$ deficient BMDM demonstrating the increased sensitivity of *Ho*$^{-/-}$ macrophages to heme induced toxicity (Figure 3F). Phagocytosis of senescent erythrocytes is the major source of heme in RPM and mouse erythrocytes have a lifespan of about 40 days (VAN PUTTEN, 1958). Notably, while RPM and BMM were absent in older (≥ 2 months) *Ho1*$^{-/-}$ *Spic*$^{igfp/igfp}$ mice they were present in younger (4–5 weeks) mice, further supporting that the loss of RPM in *Ho1*$^{-/-}$ mice is secondary to heme-induced toxicity (Figure S5C).

Heme induced loss of RPM while expanding CD11b^{hi} SPIC-EGFP ^{lo} cells. Therefore, *Spic* expression in CD11b^{hi} SPIC-EGFP ^{lo} cells may be directly induced by heme or, alternatively, may be secondary to the loss of RPM. To distinguish between these hypotheses, we treated *Ho1*$^{-/-}$ *Spic*$^{igfp/igfp}$ mice with IP heme. We reasoned that the IP administered heme will redistribute throughout the body leading to less drastic increases in heme levels within RPM and BMM compared to PHDZ or Crmp treatment, thereby mitigating cell death. IP heme robustly induced CD11b^{hi} SPIC-EGFP ^{lo} cells in the spleen and BM without significantly reducing the numbers of RPM or BMM (Figures 3G and S5B, lower panel). Furthermore, CD11b^{hi} SPIC-EGFP ^{lo} cells induced by HO1 deficiency, PDZ treatment, and heme treatment shared similar surface marker profile including high levels of TremL4 (Figure S5D). These results demonstrate a direct role of heme in the generation of CD11b^{hi} SPIC-EGFP ^{lo} cells *in vivo*.

Heme-induced CD11b^{hi} *SPIC*-EGFP ^{lo} cells are derived from monocytes

Heme-induced CD11b^{hi} SPIC-EGFP ^{lo} cells were Ly6G^{-}Ly6C$^{+/-}$ similar to monocytes (Figure 4A) and F4/80^{+}TREM^{hi} similar to RPM (Figure 4B), suggesting that CD11b^{hi} SPIC-EGFP ^{lo} cells may represent an intermediate precursor of RPM (pre-RPM) between monocyte and RPM. Consistent with this, monocytes (CD11b^{hi}Ly6C^{+}Ly6G^{-}F4/80^{-} SPIC-EGFP $^{-}$), but not neutrophils (CD11b^{hi}Ly6C^{-}Ly6G^{+}F4/80^{-} SPIC-EGFP $^{-}$) generated F4/80^{+} SPIC-EGFP $^{+}$ cells in the presence of heme *in vitro* (Figure 4C).

Conceivably, the loss of RPM (F4/80^{hi}CD11b^{lo}) and the concurrent appearance of pre-RPM (F4/80^{+} CD11b^{hi}) may reflect decreased F4/80 and increased CD11b on RPM. While this is unlikely given that pre-RPMs were induced without the loss of RPM upon IP heme treatment, we ruled out this possibility using an independent approach. BM chimeras were generated with congenically marked donor cells. Consistent with previous reports (Hashimoto et al., 2013), we observed significant persistent host contribution to the RPM pool after BM transplantation (Figure 4D). However, all pre-RPM (CD11b^{hi} F4/80^{+}) at the steady state and upon induction by Crmp were exclusively of donor origin (Figure 4D). This demonstrates that heme-induced pre-RPM are not a result of an acute loss of F4/80 and induction of CD11b on RPM, but rather are generated *de novo* from adult HSC.

We next asked whether, and under what conditions, monocytes may give rise to pre-RPM and RPM *in vivo*. Donor monocytes, like unfractionated BM cells, generated pre-RPM/RPM-like cells in the presence of hemolysis in the recipient host (Figure 4E and S6A). Donor monocytes were recovered from the recipient spleen with or without hemolysis demonstrating an equivalent ingress of the transferred monocytes (Figure S6A). However, maturation of the transferred monocytes into pre-RPM ($CD11b^{hi}$ $F4/80^{+}$) and RPM ($F4/80^{hi}VCAM1^{hi}CD11b^{lo}$) required PDZ-induced hemolysis and erythrocyte damage (Figure S6B). These results demonstrate the role of heme in generating pre-RPM and RPM from monocytes.

Heme-induced $CD11b^{hi}$ *SPIC*-EGFP ^{lo} cells give rise to RPM

To establish a developmental continuum between monocytes ($CD11b^{hi}Ly6C^{+}$ SPIC-EGFP $^{-}$), pre-RPM ($CD11b^{hi}Ly6C^{+}$ SPIC-EGFP $^{+}$), and RPM ($F4/80^{hi}CD11b^{lo}$ SPIC-EGFP ^{hi}), we compared their transcriptional profile using gene expression microarray (Figures 4F and S7A). RPM-specific genes were expressed by pre-RPM at levels intermediate between monocytes and RPM (Figure 4F). Indeed, of all genes that differ by more than 20-fold between monocytes and RPM, 94% were expressed at intermediate levels in pre-RPM (Figure S7A). Furthermore, both SPIC-$EGFP^{-}$ monocytes and SPIC-$EGFP^{+}$ pre-RPM from $Spic^{igfp/igfp}$ donors generated RPM-like cells when transferred into $Spic^{-/-}$ recipients in the presence of hemolysis, further supporting a monocyte-pre-RPM-RPM developmental continuum (Figure 4G).

Although PDZ treatment rapidly reduced the number of $F4/80^{hi}CD11b^{lo}$ RPM while expanding $F4/80^{lo}CD11b^{hi}$ pre-RPM, RPM and pre-RPM populations eventually returned to their pre-treatment frequencies suggesting that heme-induced monocyte-derived pre-RPM differentiate into RPM (Figure S7B). To examine this phenomenon further, we generated congenically marked BM chimeras. In the absence of hemolysis, a substantial fraction of RPM were of host origin, consistent with their radio-resistant property. Remarkably, hemolysis induced a complete “take over” of the RPM pool by donor-derived cells (Figure 4H). Collectively, these results strongly suggest that heme-induced pre-RPM generate RPM in the spleen.

BACH1 is a transcriptional repressor of Spic

To identify the molecular basis for heme-induced *Spic* expression, we used gene expression microarrays to compare BMDM at various times after treatment with heme (Figures 5A and 5B). Heme induced the expression of *Ho1* and *Blvrb* as well as *Slc40a1*, which encodes the mammalian iron exporter (Figure 5A), in agreement with previous reports (Delaby et al., 2008). In addition, *Spic* was induced as expected, as was *Treml4*, which can be used as a marker for RPM (Figure 5A). *Spic* was one of the most highly induced genes, and was the only transcription factor the expression of which was substantially altered (≥ 4-fold) by heme. This suggests that *Spic* expression may be induced by a heme-regulated post-transcriptional mechanism. Notably, some of the heme-induced genes, such as *Ho1*, *Gclm*, *Me1*, and *Slc7a11* were targets of the transcriptional repressor BTB and CNC homology 1 (*Bach1*) (Figures 5A and 5B) (Warnatz et al., 2011). *Bach1* and the related factor *Bach2* contain a BTB protein-protein interaction motif that mediates transcriptional repression and

a basic leucine zipper (bZIP) domain that mediates heterodimerization with other bZIP transcription factors (Oyake et al., 1996). While *Bach1* target genes were induced following heme treatment, *Bach1* expression was unchanged (Figure 5B). Compared to *Bach1*, *Bach2* expression in BMM and RPM was very low (Figure 5B).

Heme is known to inhibit BACH1 repressive activity (Ogawa et al., 2001). Notably, heme-mediated induction of SPIC-EGFP^{+} BMDM was significantly reduced with *Bach1* overexpression suggesting that *Bach1* may inhibit *Spic* expression (Figure 5C). To confirm this, we examined *Bach1*$^{-/-}$ BMDM. While *Bach1*$^{+/+}$BMDM expressed *Spic* only after heme treatment, *Bach1*$^{-/-}$ BMDM showed constitutive expression of *Spic* (Figure 5D). These results demonstrate that *Bach1* is a transcriptional repressor of *Spic* that is inhibited by heme.

Heme-mediated degradation of BACH1 induces Spic expression

Bach1 transcription was not altered by heme, suggesting post-transcriptional regulation of its activity by heme. The microRNA *miR155* has been shown to target *Bach1* (Yin et al., 2008). Therefore, we next asked if heme-mediated *Spic* induction occurs via *miR155*. RPM frequencies at the steady state as well as RPM recovery after hemolysis was normal in *miR155*$^{-/-}$ mice (Figure 6A and 6B). Importantly, heme induced robust *Spic* expression in *miR155*$^{-/-}$ BMDM (Figure 6C). These results rule out a significant role of *miR155* in heme-mediated *Spic* induction.

Heme has been suggested to induce polyubiquitination and proteasome-dependent degradation of BACH1 (Zenke-Kawasaki et al., 2007; Tan et al., 2013). Consistent with this, we observed reductions in BACH1 protein levels with increasing heme in BMDM (Figure 6D). Notably, the disappearance of BACH1 protein coincided with the appearance of a higher molecular weight band, suggesting post-translational modifications, most likely polyubiquitination (Figure 6D). Furthermore, heme-mediated induction of SPIC-EGFP^{+} BMDM was blocked by the proteasome inhibitor MG132, supporting a role for ubiquitination and proteasome based degradation of BACH1 in *Spic* induction by heme (Figure 6E).

BACH1 contains six heme-interacting cysteine-proline (CP) dipeptide motifs (Figure 6F, top) (Ogawa et al., 2001). The four carboxy-terminal CP motifs are thought to be particularly important for heme-BACH1 interaction and we mutated these four CP to Alanine-Proline (AP) in order to disrupt heme binding (Figure 6F, top) (Zenke-Kawasaki et al., 2007). As expected, the mutant BACH1 protein was resistant to heme-mediated degradation (Figure 6F, bottom). Notably, while the overexpression of WT BACH1 protein reduced the expression of SPIC-EGFP, mutant BACH1 completely blocked heme-induced SPIC-EGFP expression in BMDM (Figure 6G). This demonstrates the requirement of heme-BACH1 interactions via CP motifs for heme-mediated *Spic* expression.

BACH1 has been shown to heterodimerize with MAFK to suppress *Ho1* expression (Sun et al., 2002; Sun et al., 2004). In the absence of BACH1, MAFK heterodimerizes with the transcription activator NRF2 to activate *Ho1* expression (Sun et al., 2002; Sun et al., 2004). RPM frequency and *Spic* expression were normal in *Spic*$^{igf/igfp}$ *Nrf2*$^{-/-}$ mice suggesting that

while *Spic* and *Ho1* are both repressed by BACH1, they rely on distinct activating factors (Figure 6H). Taken together, these results demonstrate that heme-mediated induction of *Spic* proceeds via proteasome-dependent degradation of the transcriptional repressor *Bach1*, and are not dependent on *Nrf2*.

Heme-induced Bach1 inhibition promotes RPM and BMM development in vivo

RPM and BMM were present in normal frequencies in *Bach1*$^{-/-}$ mice (Figure 7A). To test for an *in vivo* role of *Bach1* in the development of RPM and BMM, we evaluated WT and *Bach1*$^{-/-}$ BM cells in an *in vivo* competitive setting. *Bach1*$^{-/-}$ BM were significantly more efficient than WT in generating RPM and BMM (Figures 7B). This effect was specific, since *Bach1*$^{-/-}$ BM was equal to WT in generating macrophages at other locations and other myeloid cells (Figures 7B and 7C). Since the competitive advantage of *Bach1*$^{-/-}$ BM in the generation of macrophages was evident only at sites of active erythrophagocytosis, RPM development may involve an additional step that is heme-dependent but *Bach1*-independent. Thus, we compared gene expression in *Bach1*$^{-/-}$ and WT BMDM in the presence or absence of heme (Figure 7D). As controls, we found that derepression of *Spic*, *Ho1*, and *SLC40A1* by heme was dependent on *Bach1* (Figure 7D). Notably, few genes were heme-induced but *Bach1*-independent, and one such gene was the RPM-associated marker TremL4 (Figures 7D and 7E). Therefore, *Bach1* inhibition at sites of erythrophagocytosis controls RPM and BMM development through derepression of *Spic*.

In summary, this study identifies the first environmental trigger inducing development of a defined tissue-specific macrophage subset. Here we showed that *Bach1* was a transcriptional repressor of *Spic* and that heme-induced proteasome-dependent degradation of BACH1 protein in monocytes led to *Spic* expression and promoted RPM and BMM development (Figure 7F). Furthermore, we showed that this pathway was important in maintaining RPM and BMM homeostasis during pathological hemolysis.

Discussion

RPM actively accrues heme via erythrophagocytosis, CD163 receptor mediated uptake of circulating hemoglobin-haptoglobin complex, and CD91 receptor mediated uptake of circulating heme-hemopexin complex (Hvidberg et al., 2005; Kristiansen et al., 2001; Bratosin et al., 1998). Therefore, hemolysis and erythrocyte damage leads to an acute buildup of heme in these cells leading to heme-induced toxicity. Such pathological conditions therefore have a ‘double impact’ on the macrophage-based iron recycling machinery: they acutely increase the quantity of heme that must be degraded but excess heme is toxic to the same macrophages that degrade this substrate. Therefore, the induction of *Spic* and pre-RPM upon increased environmental heme represents an important adaptive response during pathologic hemolysis.

Recent studies have questioned the monocyte origin of macrophages, instead suggesting that most tissue-resident macrophages are maintained by local proliferation (Schulz et al., 2012a; Hashimoto et al., 2013). Although this may be true at the steady state, our findings support a critical role for monocytes in maintaining RPM and BMM homeostasis during pathological hemolysis. Similarly, monocytes may also be critical in maintaining other tissue-resident

macrophages in response to tissue-specific insults. This suggests a dichotomy in the developmental mechanisms that maintain tissue-resident macrophages at the steady state and under pathological conditions.

Both BMM and RPM have been implicated in heme degradation and iron recycling. Our finding that these tissue-resident macrophage subsets share similar developmental pathways underscores the importance of function, rather than location, in the classification of tissue-resident macrophages. Notably, high levels of HO1 expression, similar to that in RPM, have been observed in macrophages located in human atherosclerotic plaques (Boyle et al., 2009). Therefore, macrophages that are functionally equivalent to *Spic*-dependent BMM and RPM may develop at other locations with increased environmental heme, such as those associated with hematomas and atherosclerotic plaques. In this regard, the expression of *Spic* in a small subset of liver macrophages is intriguing. Liver macrophages are also known to engulf damaged erythrocytes (Beaumont and Delaby, 2009). Therefore, SPIC-EGFP^{+} macrophages in the liver likely represents cells that actively phagocytose erythrocytes.

BACH1 degradation by heme allows its binding partner MafK to heterodimerize with NRF2 to induces *Ho1* expression (Sun et al., 2002; Sun et al., 2004). However, *Spic* induction was not dependent on *Nrf2*. Furthermore, bioinformatics analysis of the *Spic* locus did not reveal the presence of any classic MARE sequences recognized by MAF. These suggest that *Spic* regulation by BACH1 may be independent of MAFK, and that BACH1 may suppress *Spic* as a homodimer or as a heterodimer with an unknown partner.

In summary, our findings provide novel insights into iron homeostasis by linking the development of iron recycling macrophages in the spleen and BM to a molecular substrate of their metabolic function. This developmental pathway may be a paradigm for the role of tissue-specific metabolites in the maintenance of tissue resident macrophages.

Materials and Methods

Generation of *Spic*$^{igfp/+}$ mice

The details of generating the targeting construct are provided in the supplemental information. The linearized vector was electroporated into EDJ22 embryonic stem cells of 129SvEv background and targeted clones were identified by Southern blot analysis with 5′ and 3′ probes. Blastocyst injections were performed and male chimeras were bred to female 129SvEv mice.

Mice

129SvEv mice were purchased from Taconic. C57BL/6 mice and the congenic strain B6.SJL-*Ptprca Pepcb*/BoyJ (B6.SJL) were purchased from the Jackson Laboratory or NCI. *Ho1*$^{-/-}$ and *miR-155*$^{-/-}$ mice were purchased from the Jackson Laboratory. *Nrf2*$^{-/-}$ mice were kindly provided by Dr. Rajasekaran and Dr. Wang at the University of Utah. Mice were bred and maintained in our specific pathogen-free animal facility according to institutional guidelines.

Histology

Histology was performed on fixed and frozen 6–8 μm sections following established protocols as described in detail in the supplemental information.

Cell preparation

BM and peritoneal cells were harvested with Iscove's modified Dulbecco's medium (IMDM) with 10% FCS. Cells from the various organs were harvested by digesting with enzymes in IMDM following established protocols as described in detail in the supplemental information.

Flow Cytometry and Cell Sorting

Flow cytometry was performed on a FACS Canto (BD biosciences) and cell sorting performed on a FACS Aria II (BD biosciences) using well established protocols as described further in the supplemental information. All flow cytometry data were analyzed with the FlowJo software (Tree star).

Transplantation Assay

For BM chimeras, recipient mice were lethally irradiated with two staggered doses of 550 rads several hours apart and transplanted by tail vein injection with BM cells obtained from donor mice.

Monocyte transfers

Monocytes were purified by MACS based depletion and enrichment as described in the figure legends. For transfer of SPIC-EGFP^{+} and SPIC-EGFP^{-} monocytes, the MACS purified monocytes were further subjected to cell sorting. All recipient mice were treated with PDZ or PBS and some recipient mice additionally received sub-lethal radiation with a single dose of 550rad as described in the figure legends.

In vitro Cultures

BM cells were collected as described above and cultured in IMDM + 10% FCS supplemented with 20 ng/ml of GM-CSF (315-03, PeproTech), M-CSF (315-02, PeproTech), or G-CSF (300-23, PeproTech) as indicated. Unless otherwise specified, BMDM indicates the adherent BM-derived macrophages generated in the presence of 20ng/ml GM-CSF. Cells were plated at 2×10^5/ml for GM-CSF cultures and 0.5×10^6/ml for M-CSF and G-CSF cultures.

Microarray analysis

Gene expression analyses were carried out using the affymetrix platforms using standard protocols as described in the supplemental information. All data has been uploaded and made publicly available at the GEO website (GSE46983, GSE46984, and GSE53796).

Supplementary Material

Refer to Web version on PubMed Central for supplementary material.

Acknowledgments

This work was supported by the HHMI (K.M.M.), NIH AI076427-02 (K.M.M.), DOD W81XWH-09-1-0185 (K.M.M.), NIH T32 CA 9547-27 (M.H), NIH 1K08AI106953) (M.H.), and the Physician Scientist Training Program (PSTP) of the department of Pathology and Immunology at the Washington University School of Medicine (M.H.).

Reference List

Andrews NC, Schmidt PJ. Iron homeostasis. Annu Rev Physiol. 2007; 69:69–85. [PubMed: 17014365]

Beaumont C, Delaby C. Recycling iron in normal and pathological states. Semin Hematol. 2009; 46:328–338. [PubMed: 19786201]

Bemark M, Martensson A, Liberg D, Leanderson T. Spi-C, a novel Ets protein that is temporally regulated during B lymphocyte development. J Biol Chem. 1999; 274:10259–10267. [PubMed: 10187812]

Boyle JJ, Harrington HA, Piper E, Elderfield K, Stark J, Landis RC, Haskard DO. Coronary intraplaque hemorrhage evokes a novel atheroprotective macrophage phenotype. Am J Pathol. 2009; 174:1097–1108. [PubMed: 19234137]

Bratosin D, Mazurier J, Tissier JP, Estaquier J, Huart JJ, Ameisen JC, Aminoff D, Montreuil J. Cellular and molecular mechanisms of senescent erythrocyte phagocytosis by macrophages. A review. Biochimie. 1998; 80:173–195. [PubMed: 9587675]

Cambos M, Scorza T. Robust erythrophagocytosis leads to macrophage apoptosis via a hemin-mediated redox imbalance: role in hemolytic disorders. J Leukoc Biol. 2011; 89:159–171. [PubMed: 20884648]

Carlsson R, Hjalmarsson A, Liberg D, Persson C, Leanderson T. Genomic structure of mouse SPI-C and genomic structure and expression pattern of human SPI-C. Gene. 2002; 299:271–278. [PubMed: 12459275]

Cecchini MG, Dominguez MG, Mocci S, Wetterwald A, Felix R, Fleisch H, Chisholm O, Hofstetter W, Pollard JW, Stanley ER. Role of Colony-Stimulating Factor-I in the Establishment and Regulation of Tissue Macrophages During Postnatal-Development of the Mouse. Development. 1994; 120:1357–1372. [PubMed: 8050349]

Chow A, Huggins M, Ahmed J, Hashimoto D, Lucas D, Kunisaki Y, Pinho S, Leboeuf M, Noizat C, Van Rooijen N, Tanaka M, Zhao ZJ, Bergman A, Merad M, Frenette PS. CD169 macrophages provide a niche promoting erythropoiesis under homeostasis and stress. Nat Med. 2013

Chow A, Lucas D, Hidalgo A, Mendez-Ferrer S, Hashimoto D, Scheiermann C, Battista M, Leboeuf M, Prophete C, Van Rooijen N, Tanaka M, Merad M, Frenette PS. Bone marrow CD169+ macrophages promote the retention of hematopoietic stem and progenitor cells in the mesenchymal stem cell niche. J Exp Med. 2011; 208:261–271. [PubMed: 21282381]

Delaby C, Pilard N, Puy H, Canonne-Hergaux F. Sequential regulation of ferroportin expression after erythrophagocytosis in murine macrophages: early mRNA induction by haem, followed by iron-dependent protein expression. Biochem J. 2008; 411:123–131. [PubMed: 18072938]

Dranoff G, Crawford AD, Sadelain M, Ream B, Rashid A, Bronson RT, Dickersin GR, Bachurski CJ, Mark EL, Whitsett JA. Involvement of granulocyte-macrophage colony-stimulating factor in pulmonary homeostasis. Science. 1994; 264:713–716. [PubMed: 8171324]

Ganz T. Macrophages and systemic iron homeostasis. J Innate Immun. 2012; 4:446–453. [PubMed: 22441209]

Gordon S, Taylor PR. Monocyte and macrophage heterogeneity. Nature Reviews Immunology. 2005; 5:953–964.

Guillaud C, Loustau V, Michel M. Hemolytic anemia in adults: main causes and diagnostic procedures. Expert Rev Hematol. 2012; 5:229–241. [PubMed: 22475291]

Hashimoto D, Chow A, Noizat C, Teo P, Beasley MB, Leboeuf M, Becker CD, See P, Price J, Lucas D, Greter M, Mortha A, Boyer SW, Forsberg EC, Tanaka M, Van Rooijen N, Garcia-Sastre A, Stanley ER, Ginhoux F, Frenette PS, Merad M. Tissue-Resident Macrophages Self-Maintain

Locally throughout Adult Life with Minimal Contribution from Circulating Monocytes. Immunity. 2013; 38:792–804. [PubMed: 23601688]

Hemmi H, Idoyaga J, Suda K, Suda N, Kennedy K, Noda M, Aderem A, Steinman RM. A new triggering receptor expressed on myeloid cells (Trem) family member, Trem-like 4, binds to dead cells and is a DNAX activation protein 12-linked marker for subsets of mouse macrophages and dendritic cells. J Immunol. 2009; 182:1278–1286. [PubMed: 19155473]

Heng TS, Painter MW. The Immunological Genome Project: networks of gene expression in immune cells. Nat Immunol. 2008; 9:1091–1094. [PubMed: 18800157]

Hume DA. Differentiation and heterogeneity in the mononuclear phagocyte system. Mucosal Immunology. 2008; 1:432–441. [PubMed: 19079210]

Hvidberg V, Maniecki MB, Jacobsen C, Hojrup P, Moller HJ, Moestrup SK. Identification of the receptor scavenging hemopexin-heme complexes. Blood. 2005; 106:2572–2579. [PubMed: 15947085]

Itano HA, Hirota K, Hosokawa K. Mechanism of induction of haemolytic anaemia by phenylhydrazine. Nature. 1975; 256:665–667. [PubMed: 1153002]

Jenkins SJ, Ruckerl D, Cook PC, Jones LH, Finkelman FD, Van Rooijen N, MacDonald AS, Allen JE. Local macrophage proliferation, rather than recruitment from the blood, is a signature of TH2 inflammation. Science. 2011; 332:1284–1288. [PubMed: 21566158]

Kohyama M, Ise W, Edelson BT, Wilker PR, Hildner K, Mejia C, Frazier WA, Murphy TL, Murphy KM. Role for Spi-C in the development of red pulp macrophages and splenic iron homeostasis. Nature. 2009; 457:318–321. [PubMed: 19037245]

Kovtunovych G, Eckhaus MA, Ghosh MC, Ollivierre-Wilson H, Rouault TA. Dysfunction of the heme recycling system in heme oxygenase 1-deficient mice: effects on macrophage viability and tissue iron distribution. Blood. 2010; 116:6054–6062. [PubMed: 20844238]

Kristiansen M, Graversen JH, Jacobsen C, Sonne O, Hoffman HJ, Law SKA, Moestrup SK. Identification of the haemoglobin scavenger receptor. Nature. 2001; 409:198–201. [PubMed: 11196644]

Landsman L, Jung S. Lung macrophages serve as obligatory intermediate between blood monocytes and alveolar macrophages. J Immunol. 2007; 179:3488–3494. [PubMed: 17785782]

Marks SC Jr, Lane PW. Osteopetrosis, a new recessive skeletal mutation on chromosome 12 of the mouse. J Hered. 1976; 67:11–18. [PubMed: 1262696]

Murray PJ, Wynn TA. Protective and pathogenic functions of macrophage subsets. Nat Rev Immunol. 2011; 11:723–737. [PubMed: 21997792]

Ogawa K, Sun J, Taketani S, Nakajima O, Nishitani C, Sassa S, Hayashi N, Yamamoto M, Shibahara S, Fujita H, Igarashi K. Heme mediates derepression of Maf recognition element through direct binding to transcription repressor Bach1. EMBO J. 2001; 20:2835–2843. [PubMed: 11387216]

Oyake T, Itoh K, Motohashi H, Hayashi N, Hoshino H, Nishizawa M, Yamamoto M, Igarashi K. Bach proteins belong to a novel family of BTB-basic leucine zipper transcription factors that interact with MafK and regulate transcription through the NF-E2 site. Mol Cell Biol. 1996; 16:6083–6095. [PubMed: 8887638]

Pantopoulos K, Porwal SK, Tartakoff A, Devireddy L. Mechanisms of mammalian iron homeostasis. Biochemistry. 2012; 51:5705–5724. [PubMed: 22703180]

Pollard JW. Trophic macrophages in development and disease. Nat Rev Immunol. 2009; 9:259–270. [PubMed: 19282852]

Poss KD, Tonegawa S. Heme oxygenase 1 is required for mammalian iron reutilization. Proc Natl Acad Sci U S A. 1997a; 94:10919–10924. [PubMed: 9380735]

Poss KD, Tonegawa S. Reduced stress defense in heme oxygenase 1-deficient cells. Proc Natl Acad Sci U S A. 1997b; 94:10925–10930. [PubMed: 9380736]

Satpathy AT, KCW, Albring JC, Edelson BT, Kretzer NM, Bhattacharya D, Murphy TL, Murphy KM. Zbtb46 expression distinguishes classical dendritic cells and their committed progenitors from other immune lineages. J Exp Med. 2012; 209:1135–1152. [PubMed: 22615127]

Schulz C, Gomez PE, Chorro L, Szabo-Rogers H, Cagnard N, Kierdorf K, Prinz M, Wu B, Jacobsen SE, Pollard JW, Frampton J, Liu KJ, Geissmann F. A lineage of myeloid cells independent of Myb and hematopoietic stem cells. Science. 2012a; 336:86–90. [PubMed: 22442384]

Schulz S, Wong RJ, Kalish FS, Zhao H, Jang KY, Vreman HJ, Stevenson DK. Effect of light exposure on metalloporphyrin-treated newborn mice. Pediatr Res. 2012b; 72:161–168. [PubMed: 22580722]

Shibata Y, Berclaz PY, Chroneos ZC, Yoshida M, Whitsett JA, Trapnell BC. GM-CSF regulates alveolar macrophage differentiation and innate immunity in the lung through PU. 1. Immunity. 2001; 15:557–567. [PubMed: 11672538]

Sun J, Brand M, Zenke Y, Tashiro S, Groudine M, Igarashi K. Heme regulates the dynamic exchange of Bach1 and NF-E2-related factors in the Maf transcription factor network. Proc Natl Acad Sci U S A. 2004; 101:1461–1466. [PubMed: 14747657]

Sun J, Hoshino H, Takaku K, Nakajima O, Muto A, Suzuki H, Tashiro S, Takahashi S, Shibahara S, Alam J, Taketo MM, Yamamoto M, Igarashi K. Hemoprotein Bach1 regulates enhancer availability of heme oxygenase-1 gene. EMBO J. 2002; 21:5216–5224. [PubMed: 12356737]

Tan MK, Lim HJ, Bennett EJ, Shi Y, Harper JW. Parallel SCF Adaptor Capture Proteomics Reveals a Role for SCF(FBXL17) in NRF2 Activation via BACH1 Repressor Turnover. Mol Cell. 2013; 52:9–24. [PubMed: 24035498]

Taylor PR, Martinez-Pomares L, Stacey M, Lin HH, Brown GD, Gordon S. Macrophage receptors and immune recognition. Ann Rev Immunol. 2005; 23:901–944. [PubMed: 15771589]

VAN PUTTEN LM. The life span of red cells in the rat and the mouse as determined by labeling with DFP32 in vivo. Blood. 1958; 13:789–794. [PubMed: 13560578]

Warnatz HJ, Schmidt D, Manke T, Piccini I, Sultan M, Borodina T, Balzereit D, Wruck W, Soldatov A, Vingron M, Lehrach H, Yaspo ML. The BTB and CNC homology 1 (BACH1) target genes are involved in the oxidative stress response and in control of the cell cycle. J Biol Chem. 2011; 286:23521–23532. [PubMed: 21555518]

Yin Q, McBride J, Fewell C, Lacey M, Wang X, Lin Z, Cameron J, Flemington EK. MicroRNA-155 is an Epstein-Barr virus-induced gene that modulates Epstein-Barr virus-regulated gene expression pathways. J Virol. 2008; 82:5295–5306. [PubMed: 18367535]

Zenke-Kawasaki Y, Dohi Y, Katoh Y, Ikura T, Ikura M, Asahara T, Tokunaga F, Iwai K, Igarashi K. Heme induces ubiquitination and degradation of the transcription factor Bach1. Mol Cell Biol. 2007; 27:6962–6971. [PubMed: 17682061]

Research Highlights

- *Spic* regulates the development of RPM and BMM.
- Heme induces *Spic* expression in monocytes and macrophages.
- *Bach1* is a transcriptional repressor of *Spic*.
- Heme-mediated degradation of BACH1 induces *Spic* expression.

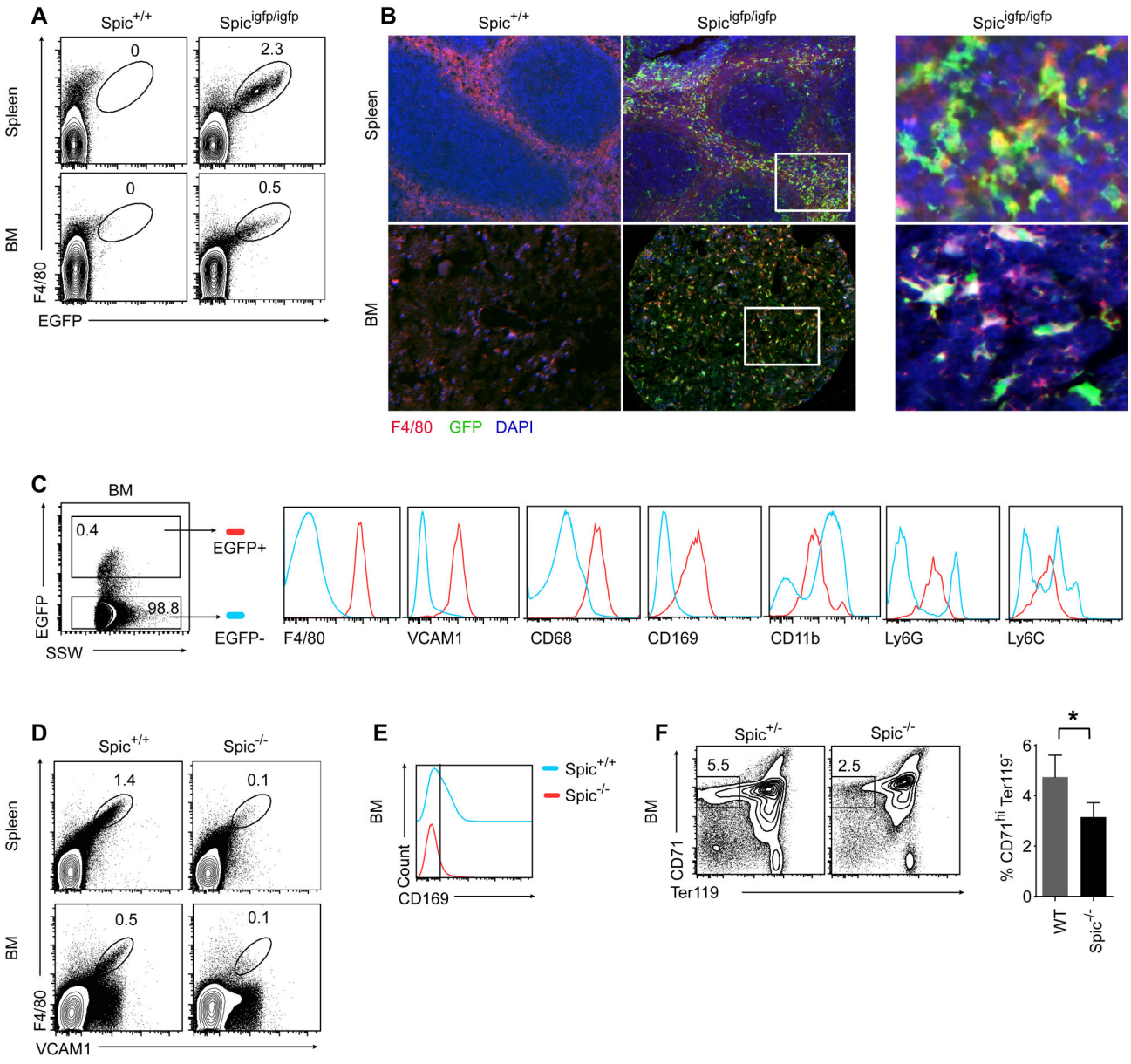

Figure 1. *Spic* is required for the development of RPM and BMM

(A) Flow cytometry with the indicated markers on Splenocytes and BM of the indicated genotypes. (B) Fixed and frozen BM and spleen sections of the indicated genotypes were stained with the indicated antibodies and DAPI (for nuclei). Right panel shows higher magnification images of indicated regions (white box). (C) Single colored histograms for the indicated markers on SPIC-EGFP^{hi} (red) and SPIC-EGFP^{-} (blue) gated *Spic*$^{igfp/igfp}$ BM cells. Ly6G and Ly6C expression within the SPIC-EGFP^{-} gate represent cells additionally gated for CD11b positivity. (D) Flow cytometry with the indicated markers on Splenocytes and BM of the indicated genotypes. (E) Single colored histograms for CD169 expression in MHC-II^{+} BM cells of the indicated genotypes. (F) Flow cytometry plots showing CD71 and Ter119 expression in CD45^{-} BM cells of the indicated genotypes. The right panel represents cumulative data from 5 mice of each genotype (bar: mean +/− S.D). * indicates statistically significant difference ($P < 0.05$, unpaired t-test). Numbers in flow cytometry plots represent percentage of cells within the indicated gates. All data in this figure is representative of ≥ 3 mice.

See also Figure S1 and S2.

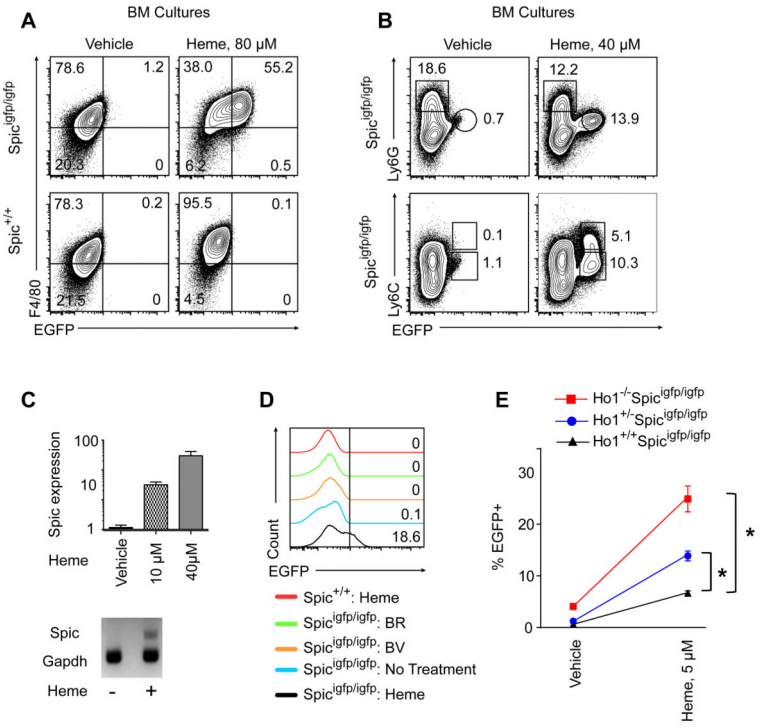

Figure 2. Heme induces *Spic* expression in macrophages generated *in vitro*

(A and B) BMDM of the indicated genotypes were treated with heme or vehicle after 6–7 days in culture. Adherent cells were harvested 2 days later and stained with the indicated markers as shown in the flow cytometry plots. (C) BMDM were treated with vehicle or increasing concentrations of heme after 6 days in culture. Adherent cells were harvested 2 days later and RNA extracted. (Top) Expression of *Spic* (Y-axis, Log_{10}) in response to vehicle or increasing levels of heme (X-axis) measured by real time quantitative PCR (bars: mean +/− S.D). Results represent two biological replicates with three technical replicates for each sample. *Spic* expression was normalized to *Hprt* and levels are relative to the expression in vehicle treated macrophages. (Bottom) Representative gel for RT-PCR products generated with the indicated primers. (D) BMDM of the indicated genotypes were treated with Heme (10 μm), biliverdin (BV, 50 μm), or bilirubin (BR, 50 μm) at the onset of culture. Cells were harvested after 8 days in culture. Shown are the single color histograms for EGFP expression in cells gated for F4/80 expression. Numbers in the flow cytometry plots represent percentage of cells within the indicated gate. All data is representative of three or more experiments with at least two replicates per group. (E) BMDM of the indicated genotypes were treated with heme or vehicle after 5 days in culture and harvested 5 days later. Shown are the percentages of $7AAD^{-}$ (live) cells expressing EGFP (bars: mean with range, n=2). * indicates statistically significant ($P < 0.05$, unpaired t-test) differences.

See also Figure S3 and S4.

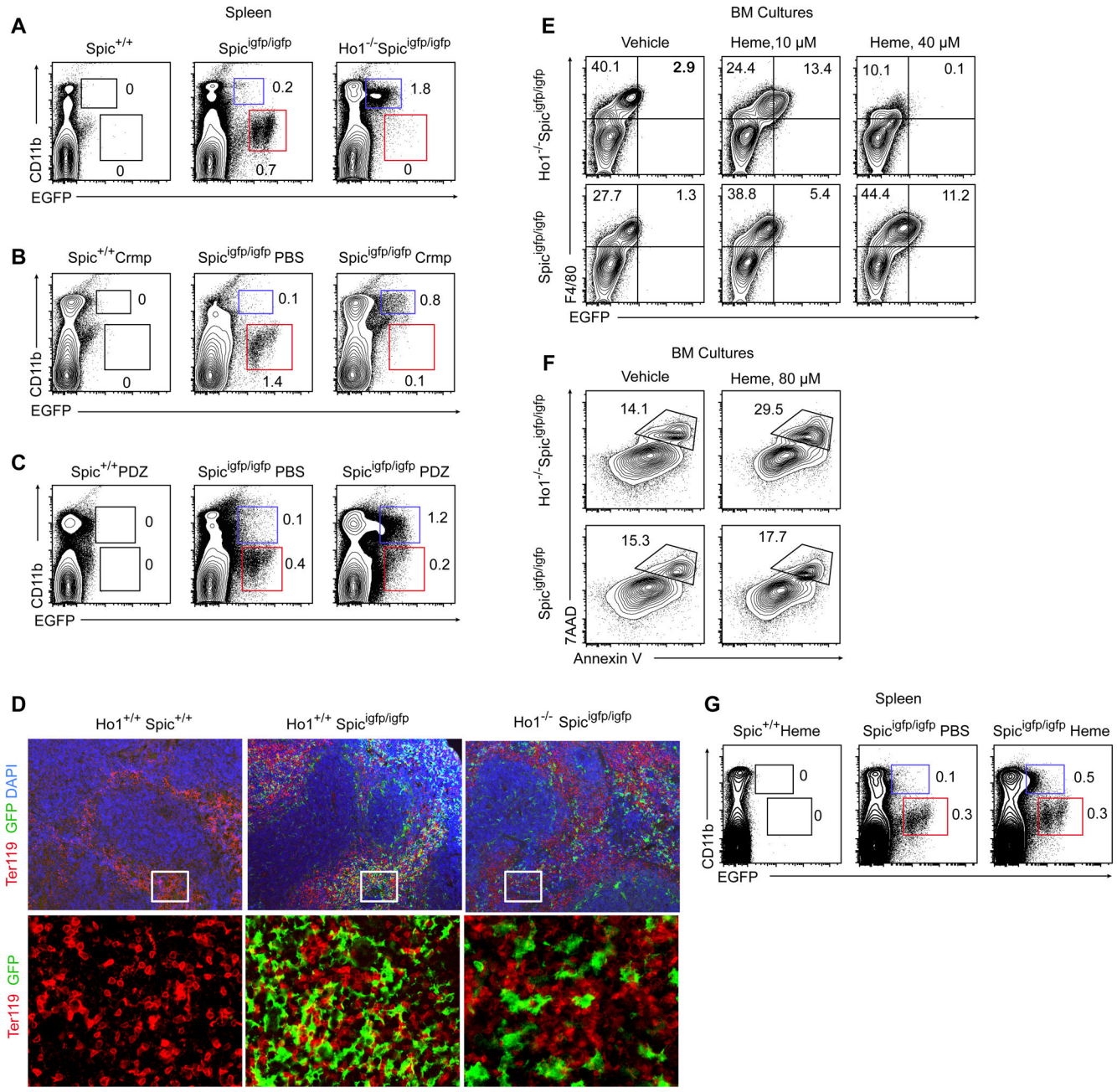

Figure 3. Heme induces *Spic* expression in myeloid cells *in vivo*

(A) Splenocytes of the indicated genotypes were stained for the indicated markers as shown in the flow cytometry plots. (B) WT and *Spic*$^{igfp/igfp}$ mice were treated intraperitoneally with 100 μl of PBS or Crmp (5 μm/kg in PBS) on three consecutive days. On day 4, splenocytes were harvested and stained for the indicated markers as shown in the flow cytometry plots. (C) WT and *Spic*$^{igfp/igfp}$ mice were treated intraperitoneally with 200 μl PBS or PDZ (2 mg in PBS) three times 48 hours apart and sacrificed 24 hr. after the final treatment. Splenocytes were harvested and stained for the indicated markers as shown in the flow cytometry plots. (D) Fixed and frozen sections of spleen of the indicated genotypes were stained with the indicated antibodies and DAPI. Lower panel shows higher magnification of the indicated regions (white box). (E) BMDM of the indicated genotypes were treated with vehicle or increasing concentrations of heme after 7 days in culture. Cells were harvested 2 days later and stained

for the indicated markers as shown in the flow cytometry plots. (F) BMDM of the indicated genotypes were treated with vehicle or high concentration of heme after 5 days in culture. Cells were harvested 24 hours later, stained for F4/80, and subsequently stained with annexin V and 7AAD. Shown are the flow cytometry plots with indicated markers on cells gated for F4/80 expression. (G) WT and *Spic*$^{igfp/igfp}$ mice were treated intraperitoneally with 200 μl of PBS or heme (0.5 mg in PBS) on three consecutive days. Splenocytes were harvested on day 4 and stained for indicated markers as shown in the flow cytometry plots. Numbers in the flow cytometry plots represent percentage of cells within the indicated gate. Red boxes represent RPM and blue boxes pre-RPM. All data in this figure is representative of two or more experiments with at least two mice or samples per group. See also Figure S5.

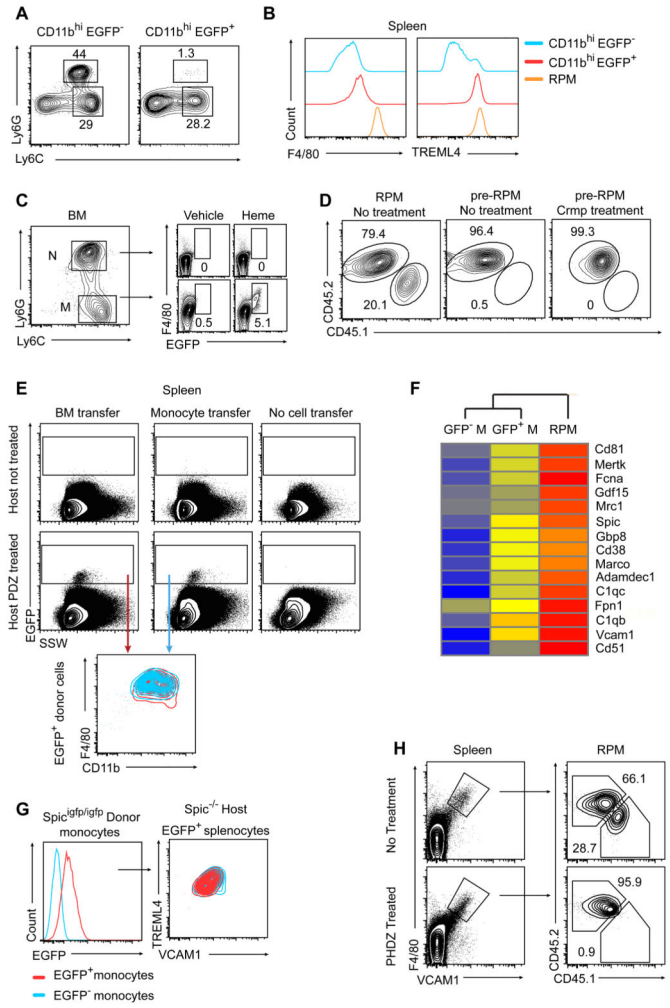

Figure 4. *Spic*$^{+}$ myeloid cells are intermediates between *Spic*$^{-}$ monocytes and *Spic*^{hi} RPM

(A, B) Splenocytes from *Spic*$^{igfp/igfp}$ and *Ho1*$^{-/-}$*Spic*$^{igfp/igfp}$ were stained for the indicated markers. (A) Flow cytometry plots with the indicated markers in CD11b^{hi} EGFP^{-} (left) and CD11b^{hi} EGFP^{+} (right) gated cells from *Ho1*$^{-/-}$*Spic*$^{igfp/igfp}$ splenocytes. (B) Single color histograms for indicated markers in CD11b^{hi}EGFP^{-} and CD11b^{hi}EGFP^{+} cells from *Ho1*$^{-/-}$*Spic*$^{igfp/igfp}$ splenocytes and CD11b^{lo}EGFP^{hi} (RPM) from *Spic*$^{igfp/igfp}$ splenocytes. (C, Left) 7AAD^{-} EGFP^{-} splenocytes pooled from 6 *Spic*$^{igfp/igfp}$ mice were selected for CD11b expression while gating out CD11c^{hi} F4/80^{hi} cells. Within these cells, monocytes (M) were sorted as Ly6G^{-}Ly6C^{+} and Neutrophils (N) as Ly6G^{+}Ly6C^{-} cells. (C, Right) Sorted monocytes and neutrophils were cultured with 5ng/ml GM-CSF with or without heme (40 μm), harvested 3 days later, and stained for markers as shown in the flow cytometry plots. (D) BM from CD45.2^{+} C57BL/6 donors were transferred into lethally irradiated CD45.1^{+} C57BL/6 recipients and splenocytes harvested after 8 weeks. Shown are the flow cytometry plots indicating donor and host derived F4/80^{hi} CD11b^{lo} RPM (Left) and F4/80^{+}CD11b^{hi} pre-RPM (middle). The plot on the right shows the same for pre-RPM induced by Crmp (5 μm/kg in 150 μl PBS, twice 24 hours apart) in the BM chimeras. (E) Monocytes were purified from 129SvEv *Spic*$^{igfp/igfp}$ splenocytes by depleting Ly6G^{+} granulocytes and enriching for CD11b^{+} cells using MACS microbeads. 129SvEv *Spic*$^{+/+}$ recipient mice were irradiated once with 550 rad followed by single treatment with 200 μl of intra-peritoneal PBS or PDZ (2 mg in PBS). About 2×10^{6} monocytes were injected (IV) into recipient mice 24 hours later. Some recipient mice were injected with about 4×10^{6} unfractionated 129SvEv *Spic*$^{igfp/igfp}$ BM cells (instead of monocytes). 4 days after the cell transfers, recipient splenocytes were stained for markers as shown in the flow cytometry plots. The dual colored flow cytometry

plot at the bottom displays the overlapping pattern of F4/80 and CD11b expression between BM and monocyte derived SPIC-EGFP^{+} cells in the host spleen. (F) Monocytes (CD11b^{hi}Ly6C^{+} SPIC-EGFP $^{-}$), pre-RPM (CD11b^{hi}Ly6C^{+} SPIC-EGFP $^{+}$), and RPM (F4/80^{hi}CD11b^{lo} SPIC-EGFP ^{hi}) were sorted from *Spic*$^{igfp/+}$ mice. RNA was extracted from the sorted cells and gene expression analysis carried out using the affymetrix expression platform. Shown is a heat map representing expression levels for selected RPM-specific genes. (G) 129 SvEv *Spic*$^{igfp/igfp}$ mice were treated with 200 μl PDZ (2 mg in PBS). Splenocytes were harvested 48 hours later and enriched for CD11b^{+} cells using MACS magnetic microbeads. Ter119^{-}Ly6G^{-}F4/80^{-}CD3^{-}B220^{-}CD11b^{+} cells from this CD11b enriched fraction were sorted into SPIC-EGFP^{+} and SPIC-EGFP^{-} cells (Left). About 2×10^{6} SPIC-EGFP^{-} and 1×10^{6} SPIC-EGFP^{+} cells were injected (IV) into 129SvEv *Spic*$^{-/-}$ recipients. Splenocytes from the recipients were harvested 4 days later. The dual colored flow cytometry plot on right displays the overlapping pattern of TREML4 and VCAM1 expression between SPIC-EGFP^{+} and SPIC-EGFP^{-} donor derived cells. (H) Lethally irradiated CD45.1^{+} C57BL/6 mice were transplanted with CD45.2^{+} C57BL/6 BM cells and treated with two doses (48 hours apart) of 200 μl of PBS or PDZ (2 mg in PBS) 5 weeks after radiation. 4 weeks after treatment, splenocytes from the recipients were stained for the indicated markers as shown in the flow cytometry plots. Numbers in the flow cytometry plots represent percentage of cells within the indicated gate. The data is representative of two or more experiments with at least two mice per group.

See also Figure S6 and S7.

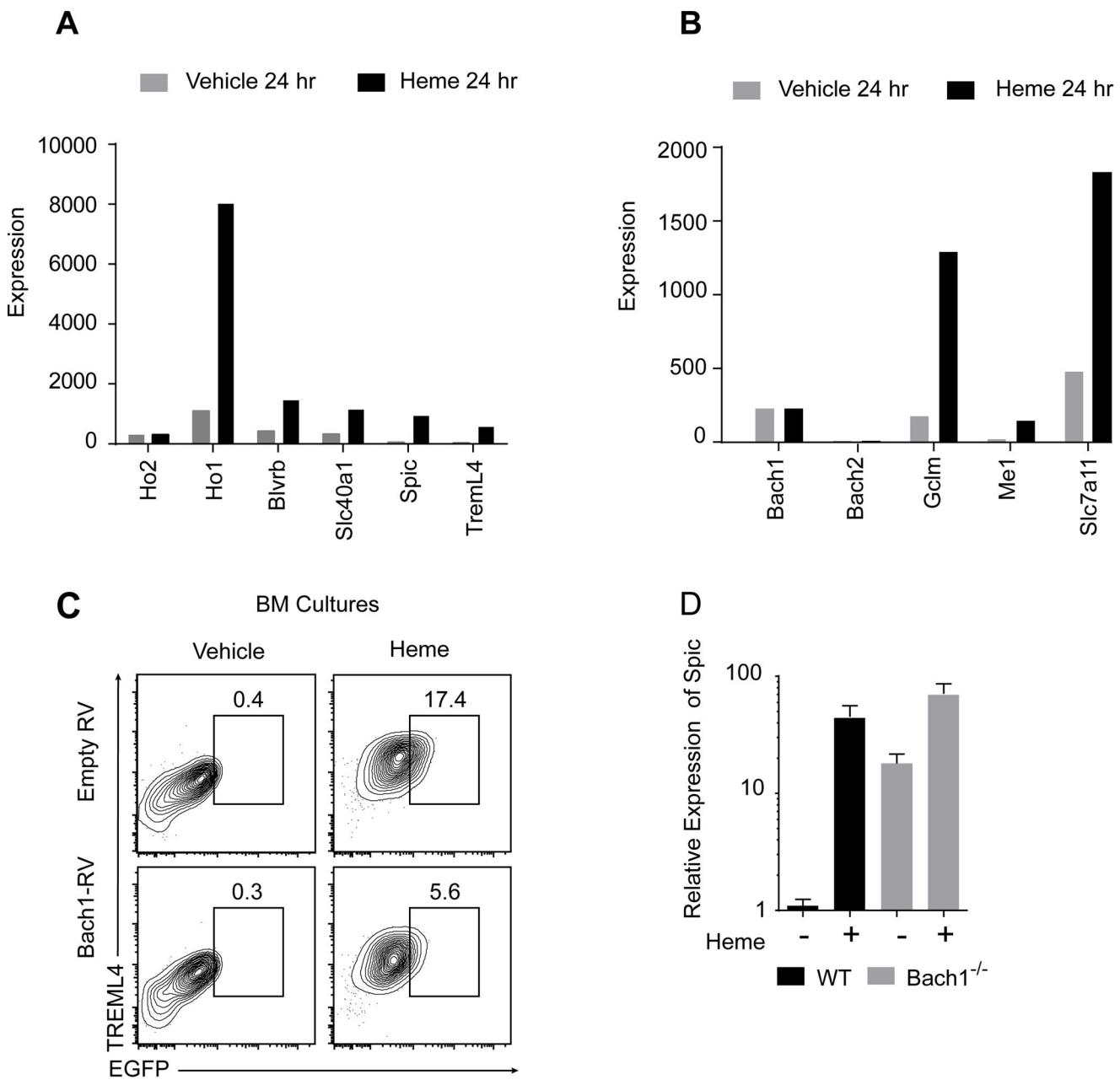

Figure 5. ***Bach1*** **is a repressor of** ***Spic expression.***

(A, B) *Spic*$^{igfp/igfp}$ BMDM were treated with heme (80 μm) or vehicle after 6 days in culture and harvested 24 hr. after treatment. RNA was extracted and microarray analysis performed using the affymetrix 1.0 platform. Shown are the expression levels (Y axis) of selected genes in vehicle (gray bars) and heme (black bars) treated cells. (C) *Spic*$^{igfp/igfp}$ BMDM were infected with retroviruses expressing mouse *Bach1* and the human *Cd4* (Bach1-RV) or expressing only the human *Cd4* (Empty-RV). 4 days after infection, the cells were treated with heme (40 μm) or vehicle. Cells were harvested four days later and stained for the indicated markers as shown in the flow cytometry plots. Numbers in the flow cytometry plots represent percentage of cells within the indicated gate. Data is representative of two or more experiments with at least two mice or samples per group. (D) *Bach1*$^{-/-}$ BMDM were treated with heme (40 μm) or vehicle after 6 days in culture. RNA was extracted 48 hrs. later and

quantitative RT-PCR performed for *Spic* transcripts. Shown is the expression value (Y-Axis, Log_{10}) relative to vehicle treated WT cells and normalized to *Hprt* expression (bars: mean +/− S.D). Results represent two distinct biological samples with three technical replicates for each biological sample.

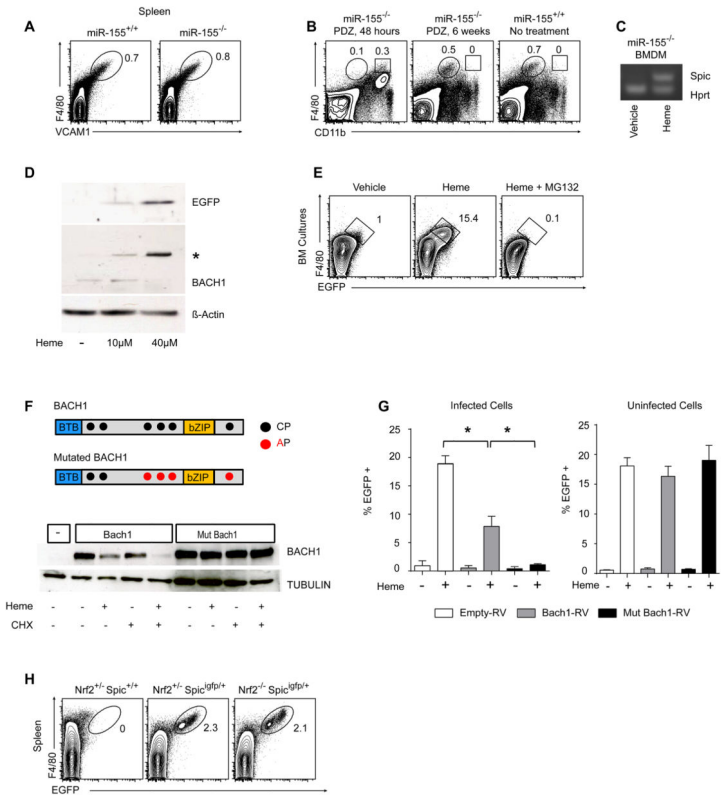

Figure 6. Heme degrades *Bach1* to de-repress *Spic* expression

(A) *miR155*$^{-/-}$ and WT splenocytes were stained for the indicated markers as shown in the flow cytometry plots. (B) *miR155*$^{-/-}$ and WT mice were treated IP with a single dose of 200 μl PBS or PDZ (2 mg in PBS). Splenocytes were harvested and stained for F4/80 and CD11b 48 hours or 6 weeks after treatment as shown in the flow cytometry plots. (C) *miR155*$^{-/-}$ BMDM were treated with heme (40 μm) or vehicle after 6 days in culture. RNA was extracted 24 hours later and RT-PCR performed with *Spic* and *Hprt* specific primers as shown in the representative agarose gel (D) *Spic*$^{igfp/igfp}$ BMDM were treated with the indicated concentrations of heme or vehicle after 7 days in culture. Cells were harvested 24 hrs. later and protein extracted. Shown are the western blots with the indicated antibodies. An anti-Bach1 reactive band appears at significantly higher molecular weight (*) in the presence of heme. (E) *Spic*$^{igfp/igfp}$ BMDM were treated with heme (40 μM), heme with the proteasomal inhibitor MG132 (10 μm), or vehicle after 7 days in culture. 2 days after treatment the cells were stained for the indicated markers as shown in the flow cytometry plots. (F) BACH1 protein contains six heme-binding Cysteine-Proline motifs (black circle), a 'repressive' BTB domain (blue box) at the N-terminus, and a basic DNA binding region preceding a protein dimerization leucine zipper domain (bZIP, orange box). Mutant BACH1 were generated by mutating the 4 Carboxy-terminal CP motifs to AP (Alanine-Proline, red circles). Human 293T cell based phoenix cells were transfected with mouse WT or mutant Bach1 expression constructs. 24 hrs. later the cells were treated with heme (40 μM) with or without cycloheximide (CHX, 25 μg/ml) to block new protein synthesis as indicated. Total protein was isolated 4 hours after treatments. Shown in the bottom panel are the western blots with the indicated antibodies. (G) *Spic*$^{igfp/igfp}$ BMDM cultures were infected with the following retroviral vectors: expressing only the human *Cd4* (empty-RV, empty bar), *Bach1* and human *Cd4* (Bach1-RV, gray bar), and mutant *Bach1* and human *Cd4* (mutant Bach1-RV, black bar). 4 days after infection, cells were treated with heme (40 μm) or vehicle. 4 days after treatment, cells were harvested and stained for hCD4 and F4/80. Within individual wells, infected cells (hCD4^{+}) were analyzed separately (Left) from uninfected (hCD4^{-}) cells (right). Shown are the percentages (Y axis) of EGFP expressing cells within F4/80^{+} gate (N = 3, bars: mean +/− S.D). * indicates statistically significant difference ($p < 0.05$, unpaired t-test). (H) Splenocytes of the indicated genotypes were stained for the indicated markers as shown in the flow

cytometry plots. Numbers in the flow cytometry plots represent percentage of cells within the indicated gate. All data in this figure is representative of two or more experiments with at least two mice or sample per group.

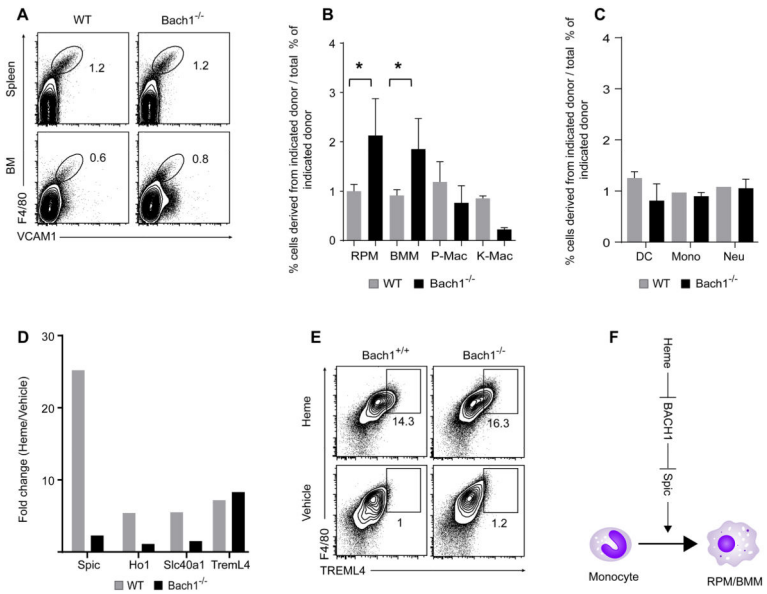

Figure 7. *Bach1* inhibition by heme induces RPM and BMM development *in vivo*

(A) WT and *Bach1*$^{-/-}$ BM and splenocytes were stained for the indicated markers as shown in the flow cytometry plots. (B–C) CD45.1^{+} C57BL/6 recipient mice were lethally irradiated and injected with a mix of CD45.2^{+} *Bach1*$^{-/-}$ and CD45.2^{+}/CD45.1^{+} WT BM cells or with a mix of CD45.2^{+} WT and CD45.2^{+}/CD45.1^{+} WT BM cells. 7–10 weeks after transplant various organs were harvested. The Y-axis represents the ratio of the percent CD45.2^{+} donor-derived (color-coded for genotype) RPM (F4/80^{hi}VCAM1^{hi}), BMM (F4/80^{hi}VCAM1^{hi}), peritoneal macrophages (P-Mac, F4/80^{hi}), kidney macrophages (K-Mac, F4/80^{hi}), Dendritic cells (DC; CD11c^{hi}MHC-II^{hi}), Monocytes (Mono; CD11b^{hi}Ly6G^{-}Ly6C^{+} in BM), and Neutrophils (Neu; CD11b^{hi}Ly6G^{+}Ly6C^{-} in BM) to the percent CD45.2^{+} of all donor derived CD45^{+} cells (bars: mean +/− S.D). * denotes statistically significant differences ($p < 0.05$, $n \geq 3$, Mann-Whitney test). (D–E) *Bach1*$^{-/-}$ BMDM were treated with heme (40 μm) or vehicle after 6 days in culture. (D) RNA was extracted 24 hrs. after treatment and microarray analysis performed using the affymetrix 1.0 platform. Shown is the fold change in expression (Y axis, $\log_2$ scale) of selected heme-inducible genes. (E) Cells were harvested 72 hrs. after treatment and stained for the indicated markers as shown in the flow cytometry plots. (F) Heme-induced development of heme-degrading macrophages.